Magnetic multilayer structures

by R. F. C. Farrow
C. H. Lee
S. S. P. Parkin

This is an overview of work at the IBM Almaden Research Center on magnetic multilayer structures comprising one, several, or many magnetic films sandwiched between nonmagnetic films. In recent years there has been increasing interest in such structures because of their novel and potentially useful properties. Recent examples of magnetic multilayer structures grown by molecular beam epitaxy (MBE) and sputtering are described. It is seen that MBE and sputtering are complementary techniques for the preparation of such structures, and that the ability to modify their magnetic properties by suitably designing their architecture is a key to their further development.

Introduction

In recent years, there has been increasing interest in magnetic multilayer structures because of their novel and potentially useful magnetic properties. In many cases, properties are observed which are unique to the architecture of the multilayer structure and have no equivalent in bulk magnetic materials.

Examples of novel properties of magnetic multilayer structures include perpendicular magnetic anisotropy in films of Fe or Co, a few monolayers in thickness, sandwiched between nonmagnetic metals or simply left uncoated in ultrahigh vacuum. A summary of work in this area has been given by Bruno and Renard [1]. In some cases, as for Co/Pt and Co/Pd multilayer structures, this perpendicular anisotropy persists to high temperatures ($\gtrsim$200°C) and has technological applications [2] in the magneto-optical storage of information. Other novel properties include the giant magnetoresistance effect in Fe–Cr multilayers [3], the antiferromagnetic coupling between Fe films through a Cr spacer film [4], and the long-range oscillatory coupling between Fe or Co films through nonmagnetic spacer films [5].

In this field, the three main methods used for the preparation of multilayer structures are MBE, conventional evaporation, and sputtering. The MBE and sputtering methods are complementary in the sense that MBE is ideally suited to film growth under controlled and monitored conditions with dynamic *in situ* analysis of film structure and composition. On the other hand, it is a much lower-throughput process than sputtering, which is well suited to the batch preparation of polycrystalline films. With sputtering one can generate large numbers of samples to explore the effects of changes in multilayer design parameters or in the materials used in multilayer formation. A key feature of MBE, however, is that by seeded epitaxy one can select specific growth axes for the multilayer structure, making it possible to investigate the dependence of its magnetic properties on orientation.

The overview presented in this paper covers work at the IBM Almaden Research Center on the preparation and properties of several types of magnetic multilayer structures, illustrating how their magnetic properties can be explored and modified by artificial layering. Following a brief description of the preparation of such structures, techniques of seeded epitaxy are described and several examples of the control of the magnetic properties of MBE-grown structures are presented. Associated, novel magnetic properties, including giant magnetoresistance and oscillatory coupling across nonmagnetic spacer films in sputtered multilayer structures, are discussed.

Preparation of magnetic multilayer structures

The two methods which are currently well suited for preparing magnetic multilayer structures are MBE and sputtering. These methods and their application to a variety of multilayer structures have been reviewed in detail elsewhere [6, 7]. In both techniques, multilayer structures are fabricated by sequential deposition onto a substrate by exposure to beams from elemental sources. Film thicknesses and deposition sequences are controlled by a computer. In deposition by MBE, use is made either of effusion sources or electron-gun evaporation sources that are fitted with computer-controlled beam shutters. Film deposition rates are typically 0.1–0.5 $Å\text{-}s^{-1}$, and the background pressure is $\sim 10^{-10}$ torr during film growth. In the case of sputtering, deposition rates are an order of magnitude greater. In the dc magnetron sputtering system used in our laboratory to generate the structures described subsequently, the background pressures prior to film growth are $\sim 10^{-9}$ torr. Consequently, in both the MBE and dc magnetron systems used in our laboratory, the incorporation of background impurities during growth is essentially negligible.

MBE and magnetron sputtering are complementary techniques for preparing magnetic multilayer structures. For example, in the case of MBE, the film growth process can be monitored in real time by RHEED (reflection high-energy electron diffraction), which permits continuous probing of the structure and orientation of a film. In addition, temporary interruption of deposition followed by transfer of the substrate, in ultrahigh vacuum, to an analysis chamber allows associated interfacial chemistry phenomena to be studied by techniques such as XPS (X-ray photoelectron spectroscopy) and XPD (X-ray photoelectron diffraction) [8]. Other *in situ* analysis probes that can be used include LEED (low-energy electron diffraction) and SAM (scanning Auger electron microscopy). **Figure 1** shows a schematic diagram of the MBE system used in our laboratory. Its various probes enable the growth process to be studied in considerable detail. In addition, the use of single-crystal substrates with clean, well-ordered surfaces makes it possible to fabricate multilayers having specific and arbitrary crystalline orientations. This is often useful in exploring structural parameters that affect magnetic properties. MBE is therefore a method ideally suited to the preparation and study of a relatively small number of single-crystal samples, one at a time. The dc magnetron sputtering process, on the other hand, is a much higher-throughput process for which the growth rate is higher than in MBE, and substrates can be loaded into the growth chamber in batches of 20 or more. It is therefore particularly well suited for generating large numbers of samples comprising different materials, and for examining the effects of incremental changes in growth and multilayer design parameters.

In dc magnetron sputtering, the pressure of the inert gas (usually argon) that is used in the growth chamber is typically a few mtorr, which precludes the use of dynamic *in situ* growth monitoring techniques such as RHEED. The argon pressure is, however, an adjustable growth parameter that influences the energy of sputtered metal atoms arriving at the substrate. Higher pressures cause thermalization of the arriving metal atoms and lead to impingement energies comparable to those of the evaporated species in MBE. The effects of growth parameters on metal–metal interfaces are complex and have been discussed elsewhere [7(b–e)]. However, a key point to note here is that sputtered multilayer structures generally contain a mixture of crystalline orientations, since the substrate has a much weaker influence on film orientation than in MBE. Indeed, in the case of MBE the substrate not only controls the orientation of a metal overlayer but may introduce chemical impurities into a film through interfacial chemical reactions. This is especially true in the case of 3D transition metals [9] and rare earths on GaAs. For this reason, it is necessary first to deposit a so-called "buffer film" of a material that is chemically stable with regard to the substrate and magnetic metal overlayer. Usually the buffer film also tends to bury impurities on the substrate and develop a smooth surface.

It is possible to control the epitaxial orientation of the buffer film by varying the substrate orientation or growth conditions. This provides a way of seeding a desired orientation of the multilayer structure. Semiconductor substrates are particularly well suited for this technique of seeded epitaxy, since they are of high structural perfection and their surfaces can be smoothed by homoepitaxy prior to metal film epitaxy. The Bragg diffraction from the substrate provides a reference for quantitative strain measurements of the multilayer. The substrates can be easily cleaved into arbitrary sizes for magnetic

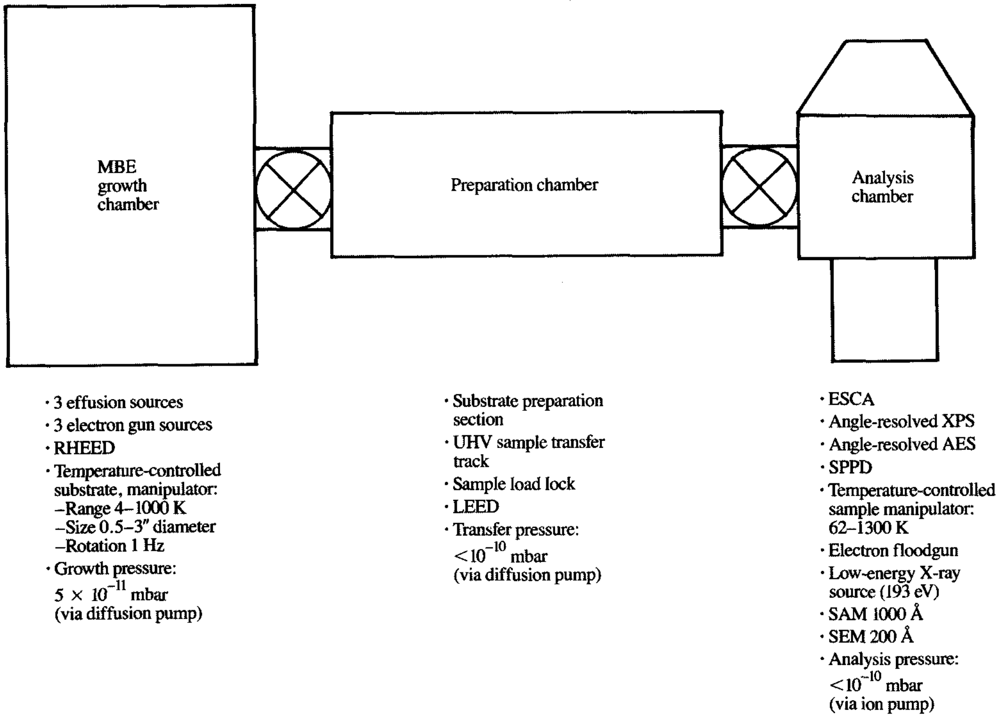

Figure 1

Schematic diagram of the MBE system used for epitaxial growth of magnetic multilayer structures. The system is configured specifically for metal multilayer growth and incorporates a variety of *in situ* structural and chemical analysis capabilities.

measurements (unlike single-crystal metals, for example). Finally, the integration of magnetic films with semiconductor substrates is of interest for potential device applications [10].

Seeded epitaxy of magnetic metals on semiconductors

For the reasons cited above, the growth by MBE of a magnetic film on a semiconductor usually requires the use of an intermediate film (a "prelayer") between the magnetic film and the semiconductor. In the case of epitaxial growth of rare-earth metals on GaAs, the authors and co-workers have found [11] that a suitable prelayer is a rare-earth fluoride, LaF_3 or NdF_3. These fluorides have hexagonal symmetry and, when grown on a GaAs $(\overline{1}\overline{1}\overline{1})$ 1×1 surface at a substrate temperature $T_s \sim 500°C$, exhibit basal plane epitaxy, with the epitaxial relationship

LaF_3 (0001), [210] ∥ GaAs $(\overline{1}\overline{1}\overline{1})$, $[\overline{1}10]$.

The in-plane misfits to GaAs are 3.6 and 1.5% for LaF_3 and NdF_3, respectively. These misfits are accommodated by interfacial edge dislocations, as illustrated by the high-resolution transmission electron micrographs (HRXTEMs) in **Figure 2**. Epitaxial overgrowth by the rare-earth metals Dy, Ho, and Er at $T_s \sim 300°C$ results [11] in basal plane epitaxy, with the epitaxial relationship

R (0001), [100] ∥ RF_3 (0001), [210].

In this setting, the in-plane misfit between the rare-earth metal and the fluoride is very large (~13%) and the interface is either semicoherent or incommensurate. In either case, grazing-incidence X-ray diffraction shows [11] that the rare-earth metal films are relaxed to their bulk lattice constant within ~25 Å from the interface. No strain can be detected in these films at room temperature. Their magnetic properties are discussed in a later section.

In the case of epitaxy of the 3D magnetic transition metals (Fe, Co) on GaAs, Ag provides a suitable prelayer, since it is thermodynamically stable in contact with GaAs and, in addition, is immiscible with Fe and Co. It is an interesting and useful fact that by varying either the method of preparation of the substrate or its orientation,

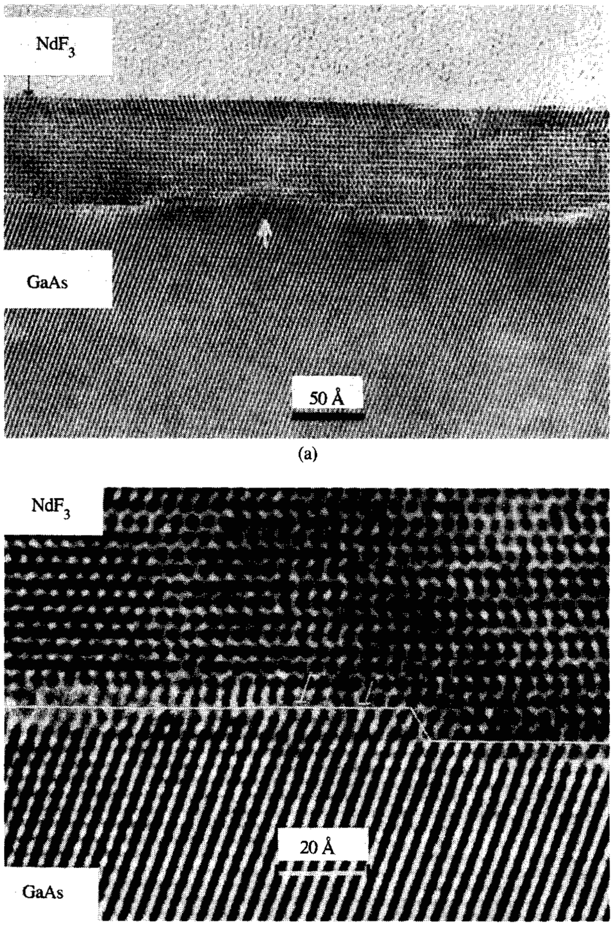

Figure 2

(a) HRXTEM image of an ~75-Å-thick film of NdF_3 grown on a GaAs $(\bar{1}\bar{1}\bar{1})$ surface. The image is viewed along the GaAs $[\bar{1}10]$ direction. Note the chemically abrupt but physically rough interface and the planarization of the NdF_3 surface. NdF_3 and LaF_3 films exhibit basal plane epitaxy on GaAs $(\bar{1}\bar{1}\bar{1})$ and can be used as seed films for rare-earth metal epitaxy. (b) Higher-magnification HRXTEM image of a region of the interface, showing a pair of interfacial misfit edge dislocations and a step in the GaAs surface. From [11(b)], reproduced with permission.

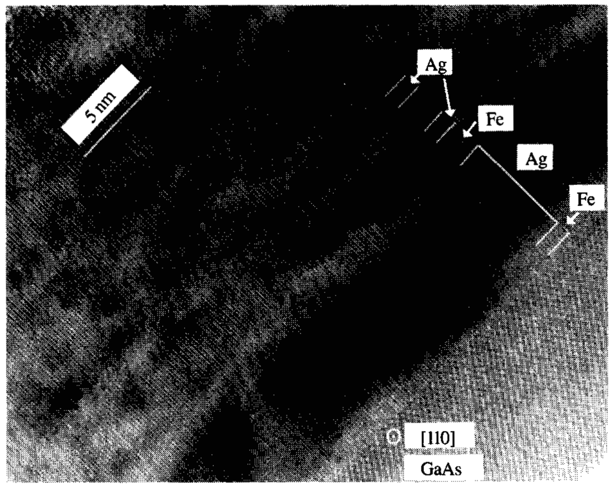

Figure 3

HRXTEM image of seeded, epitaxial Ag/Fe multilayer structure grown on a GaAs (001) surface. The section is viewed along the GaAs [110] direction. This direction is also the Fe [110] and Ag [100] direction. The structure was seeded by an ~9-Å-thick Fe prelayer followed by an ~60-Å-thick Ag film. Image recorded by C. J. Chien.

any one of the three major axes of Ag, [001], [110], or [111], can be selected as the growth axis. For example, our group has shown [12] that the predeposition of a few monolayers of Fe on the GaAs (001) surface prior to Ag epitaxy seeds the Ag [001] growth axis and results in the epitaxial relationship

Ag (001), [100] ‖ Fe (001), [110] ‖ GaAs (001), [110].

This epitaxial relationship is consistent with geometric, in-plane lattice-matching across the interfaces. For example, the lattice constant a_{Fe} of bcc Fe at room temperature is 2.866 Å, which is only 1.4% greater than 1/2 a_{GaAs}. Thus, a parallel, unrotated setting of Fe on GaAs can result in perfect in-plane registry with only a small elastic distortion of the Fe lattice. Similarly, a_{Fe} is only 0.8% less than $a_{Ag}/\sqrt{2}$. Consequently, a rotation by 45° of the Ag lattice about the [001] pole with respect to the Fe lattice can also produce a coherent interface. Overgrowth of Ag/Fe multilayers on such structures maintains this relationship throughout the layered structure, as is illustrated by the HRXTEM image in **Figure 3**. The azimuth is along the GaAs [110] direction. The lattice fringes in the Fe films represent the (110) planes. At each interface the fringe contrast switches from the characteristic stripes of ⟨110⟩ fringes in the Fe to the square lattice of ⟨200⟩ fringes in the Ag. The azimuth in Figure 3 is along the cube face normal of Ag, confirming the rotation of the Ag lattice by 45° with respect to the Fe lattice.

This seeding technique also works well with Co and permits [13] the growth of single-orientation Co/Pt multilayer structures along the Pt [001] axis. This is illustrated by the RHEED patterns in **Figure 4**. The ~12-Å prelayer adopts a body-centered tetragonal structure which is commensurate, in-plane, with GaAs, namely

Co (001), [100] ‖ GaAs (001), [100].

The Ag overlayer grows on the Co in the same orientation as on the Fe prelayer. The Pt film, which has the same fcc structure as the Ag film, grows parallel to it.

The RHEED pattern from each subsequent Co film shows that it grows in the fcc structure, parallel with the Pt. Each subsequent Pt film grows in a parallel orientation with respect to the Co and Ag films. This relationship is maintained throughout the structure to the final Pt "capping" film of the 15-period structure with 3 Å Co and 16 Å Pt, as may be seen by comparing the lower RHEED patterns. Thus, the growth axis of the entire structure is controlled by the Co and Ag prelayers.

To select Ag [110] as the growth axis, Ag was deposited directly onto the GaAs surface at $T_s \lesssim 100°C$, resulting in the epitaxial relationship

Ag (110), $[\bar{1}10]$ ∥ GaAs (001), [100].

The third major axis of Ag, Ag [111], was selected to be the growth axis by growing Ag directly on a clean GaAs $(\overline{111})$ surface at $T_s \lesssim 100°C$. The Ag [111] axis was parallel to the GaAs $[\overline{111}]$ axis, but the Ag film contained two in-plane crystallites, related by a rotation of 180° about the [111] axis. This can be described as rotational twinning with the two epitaxial relationships

Ag (111), $[0\bar{1}1]$ ∥ GaAs $(\overline{111})$, $[0\bar{1}1]$

and

Ag (111), $[\bar{1}10]$ ∥ GaAs $(\overline{111})$, $[0\bar{1}1]$.

This twinning may arise from the lack of in-plane lattice matching between Ag and GaAs across the (111) interface; the lattice misfit is ~28%.

The preceding methods result in mutually exclusive orientations of the Ag films; i.e., there is no mixing of orientations either in the Ag or the subsequent overlayers. This was confirmed by X-ray diffraction and HRXTEM experiments [13, 14]. Similar techniques may also be used to seed other orientations.

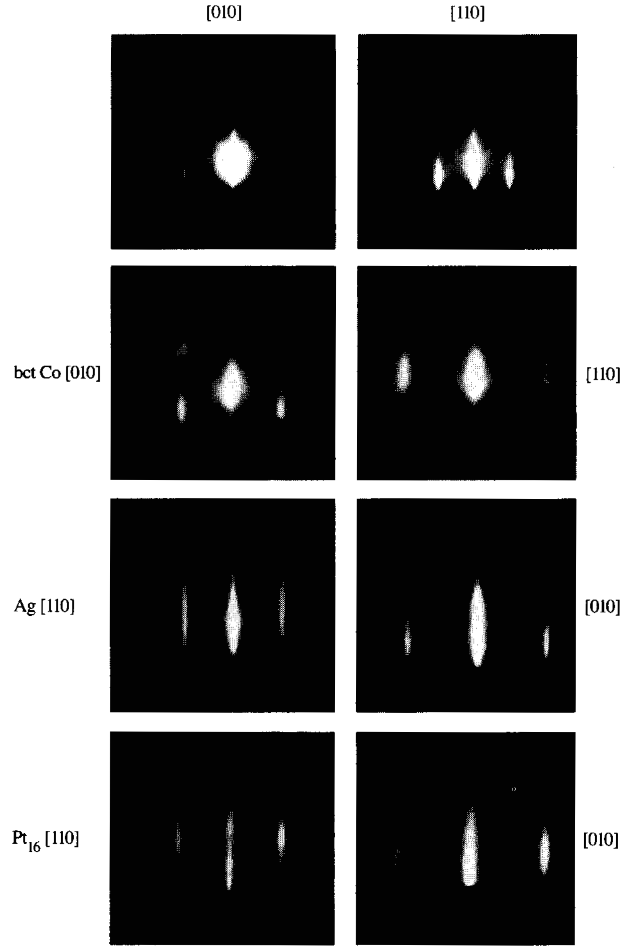

Figure 4

RHEED patterns observed during the seeded epitaxy of a 15-period Co/Pt multilayer, each period comprising a 3-Å-thick film of Co and a 16-Å-thick film of Pt. The patterns (top to bottom) were recorded on a clean GaAs (001) substrate surface: after growth of a 12-Å-thick prelayer of bct Co; after growth of an ~200-Å-thick film of Ag; and after growth of a 16-Å-thick Pt "capping" film, the sixteenth Pt film of the multilayer. From [13], reproduced with permission.

Magnetic properties of epitaxial magnetic multilayer structures on GaAs substrates

• *Rare-earth metal sandwich structures*

Strain is well known to play a major role in controlling the magnetic properties of bulk and thin-film materials. For example, magnetic anisotropy [15], magnetic moment [16], and the magnetic ordering temperature [17] are all influenced by lattice strain. In the case of epitaxial thin-film structures, lattice misfits between the nonmagnetic and magnetic films introduce coherency strains which modify the magnetic properties through magnetoelastic interactions. The family of magnetic, heavy rare earths (Gd through Tm) exhibit antiferromagnetic and ferromagnetic states which are particularly sensitive to lattice strain because of the long-range and indirect nature of the coupling between magnetic ions in the crystal. With MBE it is possible to prepare epitaxial rare-earth films with coherency strain determined by the architecture of the structure. In the case of the rare-earth metals Dy, Ho, and Er sandwiched between films of LaF_3, our group has found [11] no measurable strain at room temperature. SQUID magnetometry measurements of such films in the thickness range 25–4000 Å confirmed that the ferromagnetic ordering temperatures were close to the values for bulk crystals, although for the thinnest films (<100 Å) the transition was somewhat broadened. This broadening may be related to interfacial disorder at the lattice-mismatched interface. Recently, X-ray diffraction measurements [18] of structural and magnetic order of a 2000-Å film of Dy sandwiched

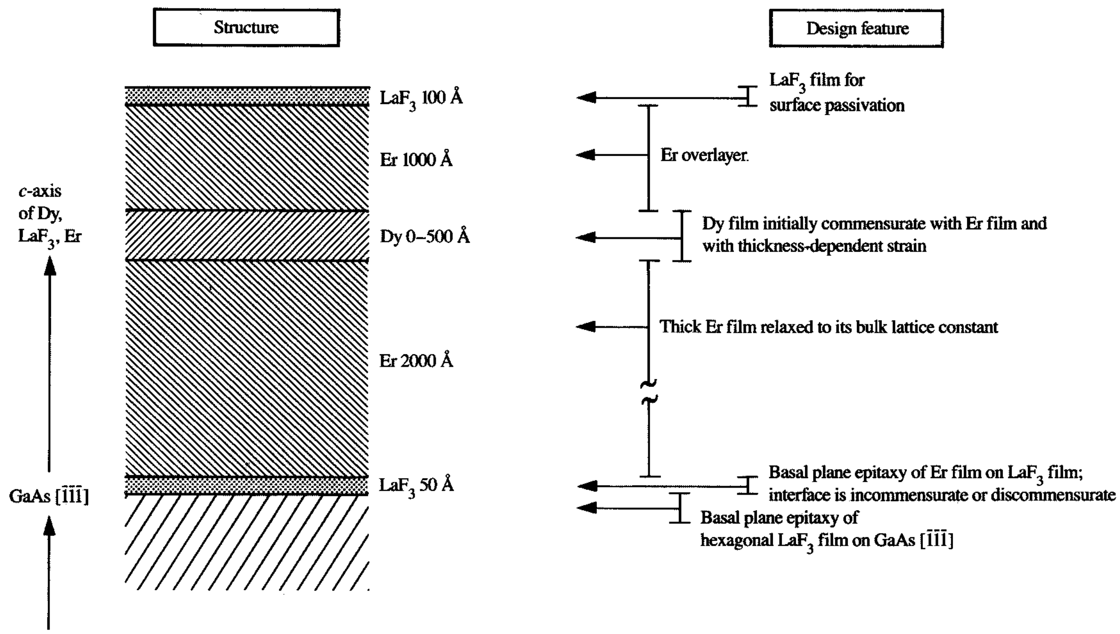

Figure 5

Schematic diagram of illustrative multilayer structure designed to introduce in-plane compressive strain in a Dy film via coherency strain induced by epitaxial growth of an Er/Dy/Er sandwich structure.

between LaF_3 films were carried out as a function of temperature on the beam line at Brookhaven National Laboratory. These studies confirmed that the ferromagnetic transition occurred close to the bulk transition temperature.

This ability of the LaF_3 prelayer to relieve misfit strain in the rare-earth films suggested a method of deliberately inducing strain in the rare-earth metals. **Figure 5** contains a schematic diagram showing an illustrative structure designed for this purpose. The intention was to impose an in-plane compressive strain on a film of the rare-earth metal Dy by sandwiching it between much thicker films of Er. The lattice misfit between Dy and Er in the basal plane is 0.89%. The element Er (a = 3.5586 Å at 25°C) has a smaller basal-plane lattice parameter than does Dy (a = 3.5903 Å at 25°C), but has the same hcp crystal structure. Thus, one expects a thin film of Dy to be subjected to in-plane compression by coherency strain. The extent to which the misfit is accommodated by interfacial misfit dislocation nucleation was not known before the method was attempted. However, such a strain-relief mechanism is known to depend on kinetic factors such as growth temperature and film growth rate. Using the method, as indicated below, the misfit was only partially relieved by misfit dislocations, and a 500-Å-thick film of Dy was subjected to a significant amount of in-plane compressive strain.

The structure was grown on the $(\bar{1}\bar{1}\bar{1})$ surface of a GaAs wafer. First, a 50-Å film of the hexagonal-structure fluoride LaF_3 was grown by sublimation of the fluoride from an effusion source. The fluoride grows with its c-axis parallel to the GaAs $[\bar{1}\bar{1}\bar{1}]$ axis and with a single in-plane epitaxial relation to the GaAs, namely

$$LaF_3\ [210] \parallel \text{GaAs}\ [\bar{1}10].$$

This epitaxial relation also holds for NdF_3 on GaAs. The NdF_3 and LaF_3 are isomorphous and can both be used as the initial film to seed the growth of the hexagonal rare-earth metals. The substrate temperature required for growth of epitaxial LaF_3 and NdF_3 is ~500°C.

The interface between the GaAs and the fluoride is chemically abrupt and semicoherent; i.e., the misfit between the GaAs and fluoride is accommodated by interfacial misfit dislocations which relax the lattice constant of the fluoride to its bulk value in a few lattice spacings. This was confirmed by *in situ* RHEED observations, grazing-incidence X-ray diffractometry, and HRXTEM. As indicated in Figure 2, the interface between

NdF_3 and GaAs $(\bar{1}\bar{1}\bar{1})$, as viewed along the GaAs [110] direction, is well defined, and the GaAs $(\bar{1}\bar{1}1)$ lattice planes terminate at a chemically abrupt but physically rough interface. The absence of interfacial chemical reactions is clear from the abrupt interface and absence of precipitates. This finding was confirmed by XPS and AES depth profiling studies of the interface. The physical roughness of the interface was due to thermal etching of the GaAs during *in situ* heat-cleaning prior to fluoride epitaxy. It is evident that the fluoride surface is less rough than the interface, suggesting that planarization occurs during growth. The higher-magnification micrograph shows individual misfit dislocations in the fluoride.

X-ray diffraction measurements [11] of strain in the structure shown in Figure 5 revealed that the Dy film was in a state of in-plane compressive strain with elastic strains:

$$\varepsilon^{\parallel} = -0.31 \pm 0.02\%$$

and

$$\varepsilon^{\perp} = +0.27 \pm 0.02\%.$$

This corresponds to in-plane compression of the Dy lattice and perpendicular Poisson dilation. On the other hand, the Er film was close to the fully relaxed state, with

$$\varepsilon^{\parallel} = +0.16 \pm 0.06\%$$

and

$$\varepsilon^{\perp} = -0.014 \pm 0.06\%.$$

Clearly, misfit dislocations have reduced but have not fully relaxed the coherency strain (maximum value $\varepsilon^{\parallel} = -0.89\%$) in the Dy film.

Interestingly, SQUID measurements for this structure showed that the ferromagnetic ordering temperature for the strained Dy films was higher than for bulk Dy. This is illustrated in **Figure 6**, which shows data for four different values of applied magnetic field along the *a*-axis (the easy axis of a bulk Dy crystal; i.e., the [100] axis). The transition from the paramagnetic to helically ordered antiferromagnetic state is evident from the cusp at about 180 K. The transition from the helically ordered state to the ferromagnetic state is field-dependent, as for bulk single crystals of Dy. The arrows indicate the onset of ferromagnetic ordering in bulk Dy. The ferromagnetic ordering in the film is in all cases completed at higher temperatures than the onset temperature for ordering in the bulk crystal. We attribute this to the imposed elastic strain in the film, since, in the bulk crystal, ferromagnetic ordering is accompanied by a discontinuous *c*-axis expansion and in-plane contraction. By mechanically imposing the structure of the ferromagnetic phase at a temperature above the Curie temperature T_c of bulk Dy, we have made it energetically favorable for ferromagnetic ordering to occur at higher temperatures. The possibility of interference from ferromagnetic ordering of the Er film is not possible since its ordering occurs at much lower temperatures (<50 K for fields below 10 kOe) than that of Dy. In addition, differential thermal expansion between Er and Dy as the film is cooled from room temperature to 100 K is less than 0.1% and would not significantly modify the much larger misfit-imposed strain in the Dy.

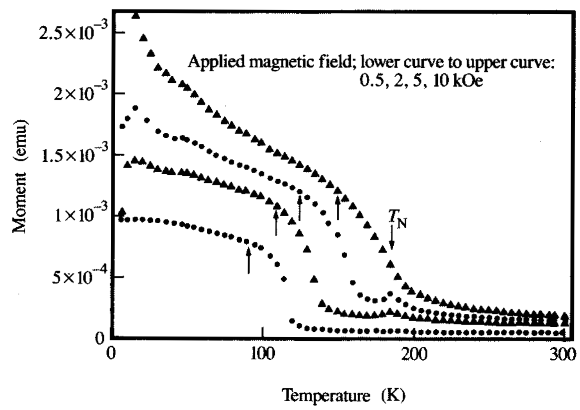

Figure 6

SQUID magnetometer data for a sandwich structure comprising GaAs $(\bar{1}\bar{1}\bar{1})$/50 Å LaF_3/2000 Å Er/500 Å Dy/1000 Å Er/1000 Å LaF_3. Note the paramagnetic-to-helical transition at 178 K and the helical-ferromagnetic transition at lower temperatures. The arrows indicate the onset of ferromagnetic ordering in bulk single crystals of Dy. For each field, ordering of the films occurred at higher temperatures than for a bulk single crystal. From [11(a)], reproduced with permission.

The opposite effect, i.e., the suppression of ferromagnetic ordering in a system with the opposite sign of misfit strain, has been demonstrated by Kwo [19]. Borchers et al. [20] have similarly shown that residual strain in even thick Er films can dramatically modify the magnetic ordering behavior, in accordance with a simple magnetoelastic model.

- *Seeded Ag/Fe sandwich structures*

Seeded epitaxy of single-crystal films of Ag grown on an Fe prelayer on GaAs (001) substrates [11] or on an Fe prelayer grown on a ZnSe film on GaAs (001) substrates [21] forms the basis for [001]-oriented Ag/Fe single or multilayer structures (see Figure 3) which exhibit perpendicular anisotropy for Fe films one to three monolayers thick. This anisotropy persists only at temperatures at or below room temperature. There is general agreement that it arises from a surface anisotropy component which competes with the demagnetizing field. The surface anisotropy increasingly dominates as the film thickness decreases. Brillouin scattering studies [22] of the surface anisotropy of Fe single crystals coated with epitaxial Ag and Au reveal a surface anisotropy of magnitude similar to that measured for the ultrathin Fe films. Moreover, the positive surface anisotropy for Ag/Fe interfaces measured from spin-wave resonance spectra in relatively thick (~900–2000 Å) epitaxial Fe films [23] is sufficient to overcome the demagnetizing field in ultrathin Fe films. Thus, the perpendicular anisotropy is an interface effect due to symmetry breaking at the interfaces rather than to an intrinsic property of ultrathin Fe films.

- *Seeded Co/Pt multilayer structures*

In the case of polycrystalline Co/Pd [24] and Co/Pt [25] multilayer structures with the Co thickness below ~10 Å, the perpendicular anisotropy persists to temperatures well above room temperature. Depending on the growth conditions, square hysteresis loops can be obtained with coercivities as high as 4 kOe. These structures also display a significant Kerr rotation (the rotation of the plane of polarization of a reflected light beam by the magnetization of the sample). These are two of the properties which are necessary for thin-film magneto-optical storage media; as a result, there is considerable current interest in the magnetic and magneto-optical properties of Co/Pt and Co/Pd multilayer structures. In magneto-optical storage media, the thin film is locally heated by a laser beam while the film is immersed in a magnetic field applied normal to its surface. If the coercivity of the film is sufficiently low at the local temperature in the beam spot, the magnetization in this spot will be switched to the field direction. Clearly, the coercivity of the unheated region of the film must remain higher than the applied field so that spots already "written" retain their original magnetization. In such applications, the Kerr effect, with the laser operating at reduced power, is used to "read" the orientation of the magnetization in the written regions. For such applications the room-temperature coercivity of the thin film should be several kOe, and the shape of the hysteresis loop should be square. Although such properties can be obtained by empirical techniques in polycrystalline multilayer films deposited by sputtering [26] or conventional evaporation [25], the origin of the anisotropy is not clear, and the mechanisms of magnetic property dependencies on growth parameters are not understood. For example, unlike the Ag/Fe structures, in which the metals are immiscible, the Co/Pt and Co/Pd systems are well known to be miscible across the entire composition range, and, in addition, the Co/Pt system has ordered phases (CoPt and $CoPt_3$). As a result, it is not clear to what extent the high-temperature perpendicular anisotropy is controlled by interfacial alloy formation.

To resolve these issues, our group has initiated [13, 14] a study of the magnetic properties of Co/Pt multilayer structures oriented along the three major axes of Pt using the techniques of seeded epitaxy outlined earlier. Structures with 15 periods of 3 Å Co and 16 Å Pt aligned along the [111] axis of Pt exhibit perpendicular anisotropy with highly square hysteresis loops and a coercive field which decreases systematically with increasing growth temperature. This is illustrated in **Figure 7**. In each case the Ag prelayer was ~200 Å thick and was grown at a substrate temperature of 100°C. The loops correspond to the use of multilayer growth temperatures of 50, 100, and 200°C, respectively. X-ray diffraction studies of these structures indicated a corresponding trend to sharper interfaces, as judged by a progressively slower fall-off in higher-order satellite intensities with increasing growth temperature. However, in all cases it was clear that interdiffusion occurred to a depth of approximately three monolayers. These results may reflect the competing effects of increasing surface mobility of adatoms with increasing growth temperature on the one hand, leading to fewer film defects and physically smoother interfaces. On the other hand, increased chemical interdiffusion and mixing is expected to occur with increasing growth temperature. Recently our group has used XPD and forward scattering to determine the extent of interfacial mixing and to explore interface crystallography [14(d)]. These techniques, which were pioneered by Fadley et al. [8], have been valuable in probing epitaxial interfaces in metal-on-metal systems such as Fe/Cu [27]. Such systems exhibit surface segregation effects in which the lowest surface-energy phase (in this case Cu) migrates to the surface of the Fe film when deposition is carried out at or above room temperature. We have found [14(d)] that the Co/Pt interfaces exhibit limited interdiffusion to the extent of approximately three monolayers.

A full account of the magnetic properties of Co/Pt multilayer structures as a function of growth axis will be presented elsewhere [13, 14]. However, it is already clear that, for structures grown along the [001] axis of Pt, the magnetic anisotropy is in-plane for 3-Å-thick Co films and 16-Å-thick Pt films. This is in strong contrast to the perpendicular anisotropy found for films of identical thickness but having a structure oriented along the [111] growth axis. XPD studies for both [001]- and [111]-oriented structures have indicated limited interfacial mixing and, in the case of the [001]-oriented structures, misfit-induced strain. Furthermore, a strong twofold, in-plane magnetic anisotropy has been found for structures grown along the [110] axis of Pt. We therefore conclude that the perpendicular anisotropy arises from magnetocrystalline anisotropy in a Co/Pt mixed interfacial region. The presence of structural defects [14(b)] and local alloy ordering in this region, combined with strain, may give rise to the differences in magnetic anisotropy among the different orientations. Fortunately, with regard to the technology of magneto-optical recording using Co/Pt multilayer structures, the preferred growth axis in polycrystalline sputtered and evaporated structures is in fact the [111] axis, which is necessary for achieving perpendicular anisotropy and square hysteresis loops.

Giant magnetoresistance in MBE-grown Fe/Cr multilayer structures

Another topical area in magnetic multilayer structures in which MBE is playing a role is the giant magnetoresistance effect, first reported [3] for MBE-grown Fe/Cr multilayer structures. The effect was observed with alternating epitaxial Fe and Cr films grown on GaAs (001) substrates [28]. If 30-Å-thick Fe films are alternated with Cr films 9–18 Å thick to form structures having 40–60 periods, a giant negative magnetoresistance results; i.e., the magnetoresistance is decreased from the zero field value by as much as 50%. Magnetometry studies show that, in zero field, the Fe films are coupled antiferromagnetically. In an applied magnetic field, this coupling is overcome, and the spins in the Fe films become aligned parallel with one another. The giant magnetoresistance effect correlates with this spin alignment behavior in that the magnetoresistance saturates at the field at which the spins are parallel. Baibich et al. [3(b)] and Camley and Barnas [29] have suggested that the giant magnetoresistance effect arises from spin-dependent transmission of the conduction electrons through the Cr films. This mechanism requires nonspecular scattering of the conduction electrons at the interfaces. If the interfaces were perfectly sharp and smooth, only specular reflection and diffraction of the electrons would occur, and this would not contribute to the magnetoresistance. The magnitude of the effect is in fact known [30] to depend on film growth parameters such as growth temperature, which may affect interface roughness and grain size. This suggests that careful studies of interface roughness as a function of growth conditions will be necessary to further the understanding of the effect.

The reason for antiferromagnetic coupling between the Fe films through the thin Cr films is not at present understood. Furthermore, recent studies by Parkin et al. [5, 30(a)] have raised new issues regarding an associated spin-density wave model. These issues are discussed in the next section.

The study of giant magnetoresistance is likely to be active for some time as the conditions for sample preparation and the physical and chemical nature of the interfaces and their influence on the coupling and transport properties are established.

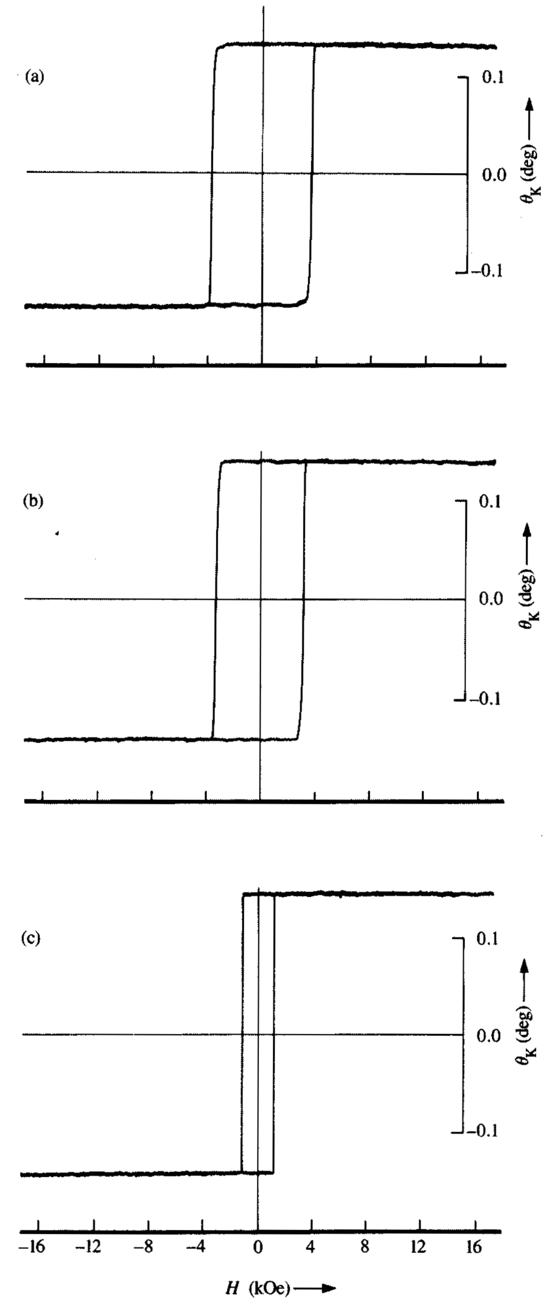

Figure 7

Hysteresis loops, recorded using polar Kerr rotation, of epitaxial Co/Pt multilayer structures comprising GaAs ($\bar{1}\bar{1}\bar{1}$)/200 Å Ag/[3 Å Co–15 Å Pt]$_{15}$/15 Å Pt. The structures were grown along the Pt [111] direction. The growth temperature of the Ag seed film was 100°C. Growth temperatures for the multilayer were (a) 50°C, (b) 100°C, and (c) 200°C. The laser wavelength was 633 nm, and the magnetic field was applied normal to the sample surface. From [14(e)], reproduced with permission.

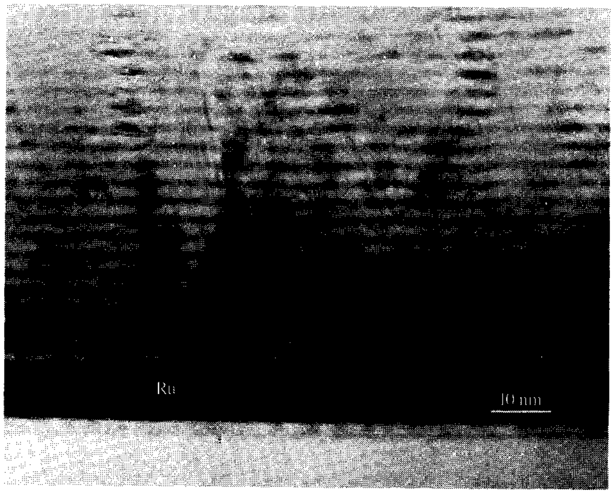

Figure 8

HRXTEM micrograph of a magnetron-sputtered Co/Ru multilayer structure comprising Si (111)/100 Å Ru/[18 Å Co/8 Å Ru]$_{20}$/50 Å Ru. The structure was deposited at a substrate temperature of 40°C. The azimuth is along the Si [11$\bar{2}$] direction. From [5], reproduced with permission.

• *Oscillations in exchange coupling and magnetoresistance in the Co/Ru, Co/Cr, and Fe/Cr multilayer structures*

Recent studies in our group [5] have shown that the giant magnetoresistance effect also occurs in magnetron-sputtered multilayer structures. Two new materials systems, Co/Ru and Co/Cr, were found to exhibit antiferromagnetic interlayer coupling and enhanced saturation magnetoresistance. **Figure 8** shows a high-resolution HRXTEM image of one of the sputtered Co/Ru multilayer structures that were examined. The substrate was a Si (111) wafer, and the cross section was viewed along the [11$\bar{2}$] direction. The structure was of the form

Si (111)/100 Å Ru/[20 Å Co/8 Å Ru]$_{20}$/50 Å Ru.

It was deposited at 40°C. The micrograph shows that the multilayer structure has surprisingly smooth and flat interfaces. Its films are contiguous over lengths greater than 0.25 μm, with no evidence of disruption. The micrograph also reveals that the structure is comprised of grains ~150 Å in size; i.e., several bilayers, within which lattice fringes are observed which are coherent across the Co/Ru interfaces. Similar micrographs of Fe/Cr multilayers showed less perfect structures with rumpled disconnected films.

Systematic studies of a large number of magnetron-sputtered samples revealed that the saturation magnetoresistance in the three materials systems did not decrease monotonically with interlayer thickness, as reported [3] for MBE-grown structures, but oscillated in magnitude as a function of interlayer thickness. Furthermore, in the three systems, the magnitude of the saturation field oscillated with the same period as that of the saturation magnetoresistance. These findings are illustrated in **Figure 9**, which shows (a) the transverse saturation magnetoresistance (at 4.2 K) and (b) the saturation field H_s (at 300 K) as a function of Ru thickness for structures of the form

Si (111)/100 Å Ru/[20 Å Co/t_{Ru}Ru]$_{20}$/50 Å Ru.

The structures were deposited at substrate temperatures of 40, 125, and 200°C, and the oscillation period was ~12–14 Å. A similar oscillatory behavior was also found for Fe/Cr and Co/Cr structures having oscillation periods of ~18 and 21 Å, respectively. Figure 9 shows that the oscillation period was not affected by the deposition temperature, but the magnitude of the saturation field was reduced significantly in the vicinity of the second oscillation. The underlying reason for this reduction is not at present understood, but is under investigation. However, the key observation of these studies is the existence of well-defined oscillations in the magnetoresistance and saturation field. The saturation field reflects the strength of the antiferromagnetic interlayer exchange coupling J_i through the expression $-4J_i = H_sMt_F$, where M and t_F are the magnetization and the thickness of the ferromagnetic film, respectively. For the Co/Ru structure with $t_{Ru} \simeq 3$ Å, the value of J_i is approximately equal to -5 erg-cm^{-2}, a very large value, two to three times larger than the largest antiferromagnetic exchange coupling values found in Fe/Cr structures. These values are so large that they clearly cannot be accounted for by magnetostatic coupling of the ferromagnetic films.

The oscillatory dependence of magnetoresistance and exchange coupling with spacer layer thickness in three different metallic multilayer material systems suggests that this is a common feature of such systems. One possible origin of the exchange coupling suggested by this work is some sort of RKKY [31] coupling, mediated by spin-polarization of the Cr or Ru films. However, such a mechanism gives rise to ferromagnetic coupling as the distance between the magnetic moments becomes very small. This appears to contradict the results for the Co/Ru structures. The data shown in Figure 9 for thicknesses of 1 and 2 Å show a low saturation field consistent with ferromagnetic coupling, probably because at such low thicknesses the Ru film is discontinuous and the Co films are directly exchange-coupled. In addition, since the period of the RKKY oscillation is tied to the Fermi wave vector, a much shorter oscillation period (~2–3 lattice spacings) would be expected instead of the 12–24-Å spacing observed. Such a short coupling length has, for example, been postulated [32] in certain spin-glass systems. Since Ru is nonmagnetic, a mechanism based on the existence of a long-range ordered magnetic state of the spacer layer seems to be ruled out. Indeed, for the Fe/Cr system an enhanced $\Delta R/R$ value and large H_s value are observed at temperatures well above the bulk Néel temperature of Cr (312 K). One might speculate that the ordering temperature of thin Cr films is substantially different from that of the bulk material, but since it is found that the antiferromagnetic exchange coupling persists up to temperatures of ~625 K, diminished in magnitude only by 30% compared to the coupling at 4.2 K, this seems unlikely. For the Co/Ru system, a larger temperature dependence of J_i is found, but again large values of J_i are found for temperatures up to 625 K.

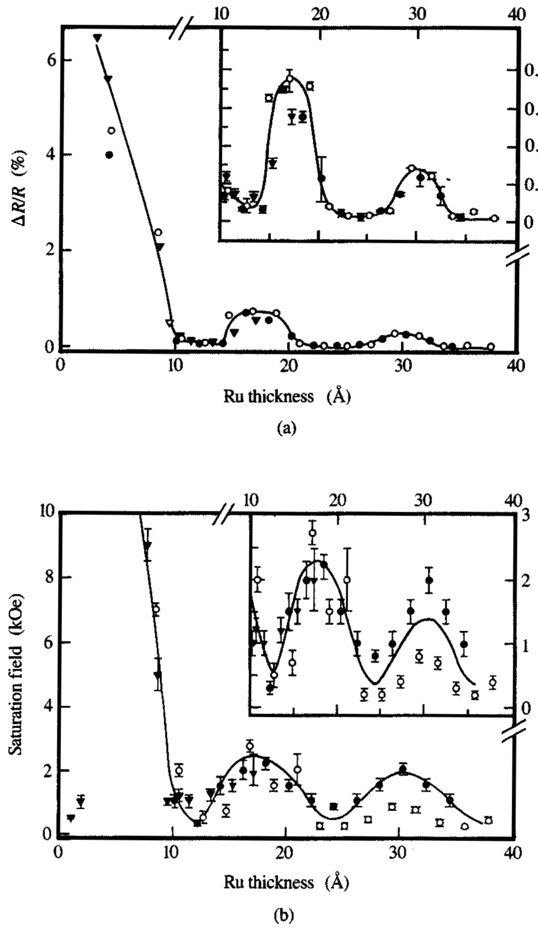

Figure 9

(a) Transverse saturation magnetoresistance (at 4.2 K) and (b) saturation field (at 300 K) versus Ru film thickness for magnetron-sputtered structure of the form Si (111)/100 Å Ru/[20 Å Co/ t_{Ru}Ru]$_{20}$/50 Å Ru. The structure was deposited at temperatures of 40°C (•), 125°C (○), and 200°C (▾). The curves are intended as a guide to the eye in representing the oscillations and do not indicate a fit to the data points. Note the significant effect of deposition temperature on saturation field for the second oscillation. From [5], reproduced with permission.

Conclusions

In this overview, we have described examples of magnetic multilayer structures that exhibit a variety of novel and potentially useful properties not found in bulk materials. In several cases, the physical mechanisms underlying these properties are not understood; in addition, they are influenced by film preparation parameters. The ability to define particular growth orientations of such structures and to probe the physical and chemical nature of their interfaces is a key advantage of MBE over more conventional deposition techniques in developing an understanding of structure-property dependences. Development of a complete understanding of interfacial phenomena in magnetic metal multilayers will require the synthesis of information from many *in situ* structural probes, including reflection high-energy electron diffraction (RHEED), low-energy electron diffraction (LEED), Auger electron spectroscopy (AES), X-ray photoelectron diffraction (XPD), and scanning tunneling microscopy (STM), as well as magnetic probes such as Kerr rotation and spin-polarized photoemission. Further advances in the understanding of the physics of low-dimensional magnetic structures and their application to devices will depend on the extent to which control and reproducibility of the interfaces of such structures can be achieved.

Acknowledgments

The authors are grateful to the Office of Naval Research for partial support of this work under Contract No. N00014-87-C-0339. They are also grateful to C. J. Chien, of the Stanford University Department of Materials Science, for the high-resolution electron microscopy studies of the magnetic multilayer structures, and to E. E. Marinero for recording the hysteresis loops shown in Figure 7.

References

1. P. Bruno and J. P. Renard, *Appl. Phys. A* **49,** 499 (1989).
2. (a) W. P. Zeper, F. J. Greidanus, P. F. Carcia, and C. R. Fincher, *J. Appl. Phys.* **65,** 4971 (1989). (b) K. Nakamura, S. Tsunashima, S. Iwata, and S. Uchiyama, *IEEE Trans. Magnetics* **25,** 3758 (1989). (c) S. Hashimoto, H. Matsuda, and Y. Ochiai, *Appl. Phys. Lett.* **56,** 1069 (1990).
3. (a) F. N. Van Dau, A. Fert, P. Etienne, M. N. Baibich, J. M. Broto, J. Chazelas, G. Creuzet, A. Friederich, H. Hurdequint, J. P. Redoules, and J. Massies, *J. de Phys.* **49,** C8-1633 (1988). (b) M. N. Baibich, J. M. Broto, A. Fert, F. Nguyen Van Dau, F. Petroff, P. Etienne, G. Creuzet, A. Friederich, and J. Chazelas, *Phys. Rev. Lett.* **61,** 2472 (1988).
4. F. Saurenbach, J. Barnas, G. Binasch, M. Vohl, P. Grunberg, and W. Zinn, *Thin Solid Films* **175,** 317 (1989).

5. S. S. P. Parkin, N. More, and K. P. Roche, *Phys. Rev. Lett.* **64,** 2307 (1990).
6. (a) R. F. C. Farrow, *J. Cryst. Growth* **104,** 556 (1990). See also Reference 23. For a general review of multilayer synthesis techniques, see *Proc. Mater. Res. Soc. Sympos.* **103,** T. W. Barbee, Jr., F. Spaepen, and L. Greer, Eds., 1988.
7. (a) R. E. Somekh, R. J. Highmore, K. Page, R. J. Home, and Z. H. Barber, *Proc. Mater. Res. Soc. Sympos.* **103,** 29 (1988). (b) E. Kay, F. Parmigiani, and W. Parrish, *J. Vac. Sci. Technol. A* **6,** 3074 (1988). (c) F. Parmigiani and E. Kay, *Appl. Phys. Lett.* **53,** 2480 (1988). (d) J. M. E. Harper, in *Plasma-Surface Interaction and Processing of Materials*, O. Auciello, Ed., Kluwer Academic Publishers, Netherlands, 1990, p. 251. (e) J. M. E. Harper, J. J. Cuomo, R. J. Gambino, and H. R. Kaufman, in *Surface Modification by Ion Bombardment: Fundamentals and Applications*, R. Kelly and O. Auciello, Eds., Elsevier, Amsterdam, 1984.
8. (a) C. S. Fadley, *Prog. Surf. Sci.* **16,** 275 (1984). (b) J. Osterwalder, E. Stewart, D. Cyr, C. S. Fadley, J. Mustre de Lyon, and J. J. Rehr, *Phys. Rev. B* **35,** 9859 (1985).
9. (a) G. A. Prinz, in *Thin Film Growth Techniques for Low-Dimensional Structures*, R. F. C. Farrow, S. S. P. Parkin, P. J. Dobson, J. H. Neave, and A. S. Arrott, Eds., *NATO ASI Series B* **163,** 311 (1987). (b) S. A. Chambers, F. Xu, H. W. Chen, I. M. Vitomirov, S. B. Anderson, and J. H. Weaver, *Phys. Rev. B* **34,** 6605 (1986).
10. G. A. Prinz, *Science* **250,** 1092 (1990).
11. (a) R. F. C. Farrow, S. S. P. Parkin, V. S. Speriosu, A. Bezinge, and A. Segmuller, *Proc. Mater. Res. Soc. Sympos.* **151,** 203 (1989). (b) C. J. Chien, R. F. C. Farrow, and J. C. Bravman, *Proc. Mater. Res. Soc. Sympos.* **160,** 513 (1990).
12. R. F. C. Farrow, V. S. Speriosu, S. S. P. Parkin, C. J. Chien, J. C. Bravman, R. F. Marks, P. D. Kirchner, G. A. Prinz, and B. T. Jonker, *Proc. Mater. Res. Soc. Sympos.* **130,** 281 (1989).
13. C. H. Lee, R. F. C. Farrow, C. J. Lin, E. E. Marinero, and C. J. Chien, *Phys. Rev. B: Rapid Commun.* **42,** 11384 (1990).
14. (a) C. H. Lee, R. F. C. Farrow, B. D. Hermsmeier, R. F. Marks, W. R. Bennett, C. J. Lin, E. E. Marinero, P. D. Kirchner, and C. J. Chien, *J. Mag. & Magn. Mater.* (1991, in press). (b) C. J. Chien, R. F. C. Farrow, C. H. Lee, C. J. Lin, and E. E. Marinero, *J. Mag. & Magn. Mater.* (1991, in press). (c) C. J. Lin, G. L. Gorman, C. H. Lee, R. F. C. Farrow, E. E. Marinero, H. V. Do, H. Notarys, and C. J. Chien, *J. Mag. & Magn. Mater.* (1991, in press). (d) B. D. Hermsmeier, R. F. C. Farrow, C. H. Lee, E. E. Marinero, C. J. Lin, R. F. Marks, and C. J. Chien, Proceedings of the 35th Annual Conference on Magnetism and Magnetic Materials, San Diego, CA, October 29–November 1, 1990. To be published in *J. Appl. Phys.* **69** (April 1991). (e) R. F. C. Farrow and C. H. Lee, *Proc. Mater. Res. Soc. Sympos.* **187,** 211 (1991).
15. G. F. Dionne, *Mater. Res. Bull.* **6,** 805 (1971).
16. O. K. Andersen, J. Madsen, U. K. Poulsen, O. Jepsen, and J. Kollar, *Phys. B+C* **86–88,** 249 (1977).
17. B. Coqblin, *The Electronic Structure of Rare Earth Metals and Alloys: The Magnetic Heavy Rare Earths,* Academic Press, Inc., New York, 1977.
18. R. F. C. Farrow, M. F. Toney, B. D. Hermsmeier, S. S. P. Parkin, and D. G. Wiesler, Proceedings of the 35th Annual Conference on Magnetism and Magnetic Materials, San Diego, CA, October 29–November 1, 1990. To be published in *J. Appl. Phys.* **69** (April 1991).
19. J. R. Kwo, in *Thin Film Growth Techniques for Low-Dimensional Structures*, R. F. C. Farrow, S. S. P. Parkin, P. J. Dobson, J. H. Neave, and A. S. Arrott, Eds., *NATO ASI Series B* **163,** 337 (1987).
20. J. A. Borchers, M. B. Salamon, R.-R. Du, and C. P. Flynn, Paper R 5.7, presented at meeting of American Physical Society, Anaheim, CA, March 16, 1990. See also R. W. Erwin, J. J. Rhyne, J. Borchers, M. B. Salamon, R. Du, and C. P. Flynn, *Proc. Mater. Res. Soc. Sympos.* **166,** 133 (1990).
21. (a) N. C. Koon, B. T. Jonker, F. A. Volkening, J. J. Krebs, and G. A. Prinz, *Phys. Rev. Lett.* **59,** 2463 (1987). (b) J. J. Krebs, B. T. Jonker, and G. A. Prinz, *J. Appl. Phys.* **63,** 3467 (1988). (c) F. A. Volkening, B. T. Jonker, J. J. Krebs, N. C. Koon, and G. A. Prinz, *J. Appl. Phys.* **63,** 3869 (1988).
22. J. R. Dutcher, J. F. Cochran, B. Heinrich, and A. S. Arrott, *J. Appl. Phys.* **64,** 6095 (1988).
23. R. F. C. Farrow, *J. Appl. Phys.* **64,** 5315 (1988).
24. F. J. A. den Broeder, D. Kuiper, H. C. Donkersloot, and W. Hoving, *Appl. Phys. A* **49,** 507 (1989).
25. F. J. A. Greidanus, W. B. Zeper, F. J. A. Den Broeder, W. F. Godlieb, and P. F. Carcia, *Appl. Phys. Lett.* **54,** 2481 (1989).
26. N. Sato, *J. Appl. Phys.* **64,** 6424 (1988).
27. D. A. Steigerwald and W. F. Egelhoff, Jr., *Surf. Sci.* **202,** 472 (1988).
28. P. Etienne, G. Creuzet, A. Friederich, F. Nguyen-Van-Dau, and A. Fert, *Appl. Phys. Lett.* **53,** 162 (1988).
29. R. E. Camley and J. Barnas, *Phys. Rev. Lett.* **63,** 664 (1989).
30. (a) S. S. P. Parkin, S. Fan, N. More, and K. P. Roche, Paper HA-04, presented at the 34th Annual Conference on Magnetism and Magnetic Materials, Boston, MA, November 28–December 1, 1989. Abstract published in *J. Appl. Phys.* **67,** 5931 (1990). (b) A. Fert, A. Barthelemy, M. N. Baibich, S. Hadjoudj, P. Etienne, R. Cabanel, S. Lequien, F. Nguyen Van Dau, and G. Creuzet, Paper HA-01, presented at the 34th Annual Conference on Magnetism and Magnetic Materials, Boston, MA, November 28–December 1, 1989. *J. Appl. Phys.* **67,** 5908 (1990).
31. Y. Yafet, *J. Appl. Phys.* **61,** 4058 (1987).
32. See for example *Metallic Glasses*, by K. Moorjani and J. M. D. Coey, Elsevier, Amsterdam, 1984.

Received May 15, 1990; accepted for publication October 25, 1990

Robin F. C. Farrow *IBM Research Division, Almaden Research Center, 650 Harry Road, San Jose, California 95120.* Dr. Farrow is a Research Staff Member in the Physical Sciences Department at the Almaden Research Center. He received his B.Sc and Ph.D in physics from Queen Mary College, University of London (UK), in 1964 and 1970, respectively. His career began in 1968 at the Royal Signals and Radar Establishment in the UK, where he studied the growth of silicon films from molecular beams of silane. From 1968 to 1982, Dr. Farrow developed and extended the technique of MBE (molecular beam epitaxy) to a wide range of materials including InP, metals, fluorides, II–VI compounds, and metastable phases. Since joining IBM in 1985, he has pursued an interest in the relationship between structural and magnetic properties of well-characterized epitaxial films of transition metals and rare earths. Dr. Farrow is a member of the American Physical Society, the European Physical Society, and the Materials Research Society.

Charles H. Lee *IBM Research Division, Almaden Research Center, 650 Harry Road, San Jose, California 95120.* Dr. Lee received a B.S. in physics from Tamkang University, Taiwan, in 1981. He received a Ph.D. in physics and electrical engineering from Arizona State University in 1987. From May 1987 to August 1989, Dr. Lee was a Research Associate in the Physics Department of the University of Michigan, working on magnetic superlattices. He subsequently joined IBM at the Almaden Research Center as a Visiting Scientist in the Materials Research Department to work on magnetic thin films and superlattices. Dr. Lee is a member of the American Physical Society and the Materials Research Society.

Stuart S. P. Parkin *IBM Research Division, Almaden Research Center, 650 Harry Road, San Jose, California 95120.* Dr. Parkin is currently a Research Staff Member at the IBM Almaden Research Center. He was elected to a Research Fellowship at Trinity College, Cambridge, in 1979 and received his Ph.D. a year later. His work at the Cavendish Laboratory, Cambridge, involved studies of the structural and physical properties of a family of layered magnetic compounds. After a Royal Society European Exchange Fellowship at the Laboratoire de Physique des Solides, Orsay, France, he joined the IBM Almaden Research Center in 1982. Dr. Parkin was part of the team that discovered a new class of organic superconductors (based on the BEDT–TTF molecule) in 1983. More recently, his interests have centered on the growth and properties of ultrathin magnetic films and superlattices. This work includes studies of the magnetization profiles of thin magnetic films using polarized neutron reflectometry and finite size effects on the magnetic properties of ultrathin antiferromagnetic films. He also recently discovered oscillations in the giant magnetoresistance and interlayer exchange coupling in a large number of magnetic multilayer systems, part of which work is described in this paper. Dr. Parkin has also worked extensively on high-critical-temperature superconductors, receiving an IBM Outstanding Technical Achievement Award in 1989 for that work.